Pedosphere **36**(2): 460–473, 2026
doi: 10.1016/j.pedsph.2024.12.007
ISSN 1002-0160/CN 32-1315/P

Published by Elsevier B.V. and Science Press

PEDOSPHERE

www.elsevier.com/locate/pedosphere

Mechanism of biochar decomposition mediated by bacteria shifts the molecular structure of soil organic matter to high-molecular-mass aromatic components

Xu CHEN, Xiaozeng HAN, Wenxiu ZOU, Jun YAN and Xinchun LU*

Key Laboratory of Mollisols Agroecology, Northeast Institute of Geography and Agroecology, Chinese Academy of Sciences, Harbin 150081 (China)

(Received September 26, 2024; revised December 2, 2024; accepted December 20, 2024)

ABSTRACT

The interaction between biochar amendments and soil dissolved organic matter (DOM) is crucial for soil health and carbon (C) sequestration, yet the molecular mechanisms underlying these effects are not fully understood. This study employed ultrahigh-resolution Fourier transform ion cyclotron resonance mass spectrometry to comprehensively assess the influence of biochar on the chemodiversity of DOM at a molecular level, with a particular focus on the interactions between bacterial species and DOM molecules. A five-year field experiment was conducted, involving four treatments, no fertilization (NF), conventional fertilization (CF), conventional fertilization with low-rate biochar at 15 000 kg ha^{-1} (LB), and conventional fertilization with high-rate biochar at 60 000 kg ha^{-1} (HB). Biochar amendment, while increasing soil pH and nutrient contents, stimulated bacterial diversity and abundance, particularly at the higher application rate. Specifically, bacterial abundance increased by 58.0%, 130.9%, and 272.8% in CF, LB, and HB treatments, respectively, compared to NF, while bacterial diversity was also notably lower in both NF and CF than in HB. Furthermore, biochar amendment lowered the chemodiversity and thermodynamic stability of DOM by shifting its composition toward more aromatic molecules that contain more C, less C saturation, and higher molecular mass, ultimately increasing the retention of DOM. Further analysis of the molecular composition of DOM indicated that the overall increase in molecular mass was primarily due to increases in high-molecular-mass C-hydrogen (H)-oxygen (O)-nitrogen (N) and CHO compounds. Keystone bacterial taxa in the biochar-amended co-occurrence networks were also the most closely connected with the CHO and CHON compounds. These compounds exhibited similar, narrow O/C and H/C ratios within the high-molecular-mass range, and their positive correlations were approximately twice as strong as the negative correlations. These results together suggest that biochar amendment leads to the homogenization of the DOM pool, with its molecular characteristics being shaped more by bacterial contributions than by their consumption.

Key Words: bacterial community, biodiversity, chemodiversity, dissolved organic matter, soil amendment, soil microbiome

Citation: Chen X, Han X Z, Zou W X, Yan J, Lu X C. 2026. Mechanism of biochar decomposition mediated by bacteria shifts the molecular structure of soil organic matter to high-molecular-mass aromatic components. *Pedosphere*. **36**(2): 460–473.

INTRODUCTION

The use of biochar as a soil amendment is emerging as a valuable strategy for climate change mitigation by increasing soil organic matter (SOM) and reducing soil carbon (C) emissions (Wang *et al*., 2023). The application of biochar releases a soluble fraction of organic material (Ling *et al*., 2022), which is an essential component of dissolved organic matter (DOM) in the soil environment. This organic fraction affects various environmental geochemical processes, including alterations to soil constituents and the cycling of elements. Nonetheless, the effects of biochar application can be highly nuanced and depend greatly upon specific conditions. For example, its impact on plant-derived C decomposition can vary greatly: some studies have reported decreased rates of decomposition (Weng *et al*., 2017), whereas others have reported higher C losses in biochar-amended soils (Fu *et al*., 2022). These findings underscore the need for careful consideration and effective management to maximize the benefits of biochar while mitigating potential drawbacks in agricultural applications.

Biochar has been extensively researched for its immediate impact on soil properties and crop growth in short-term experiments, usually with annual additions (Ling *et al*., 2022). However, extrapolating these findings to field-scale conditions involving long-term biochar aging, complex plant-soil-microbe interactions, and the transformation of DOM through processes like sorption and leaching remains challenging (Underwood *et al*., 2019). In agricultural production, biochar is typically reapplied only after several years due to its long-term stability and higher cost compared with traditional amendments such as compost or manure. Frequent application of biochar may help maintain a steady release of nutrients into the soil and increase their availability for crops, but it can potentially obscure the processes and characteristics of biochar transformation in the soil, especially when application intervals are short. The effects of each subsequent application can overlap with remnants

*Corresponding author. E-mail: luxinchun@iga.ac.cn.

from previous ones, making it difficult to distinguish the individual contributions of each batch and thereby limiting a precise understanding of its influence on soil improvement and nutrient dynamics. Several relatively short-term studies involving annual supplementation have examined its influence on the attributes of DOM (Feng *et al*., 2021; Han *et al*., 2024), but the abundance and molecular-level attributes of DOM from agricultural land under long-term biochar amendment have not been extensively investigated.

Dissolved organic matter is a small fraction of SOM, yet it represents the most dynamic and readily available organic component in soil. The heterogeneity of DOM, while effectively representing its contents, constrains accurate assessment of the quality of its chemical composition. Investigating the chemodiversity of DOM, which describes the varied chemical compositions and characteristics of DOM molecules, has attracted substantial research attention due to its potential to provide insights into biogeochemical processes in soil (Li *et al*., 2018; Ding *et al*., 2020). The changes in DOM chemodiversity induced by biochar are primarily driven by alterations in the soil microbiome (Chen *et al*., 2019). By selectively degrading specific SOM fractions, the microbial community affects molecular diversity and DOM decomposition and likely contributes to the accumulation of new organic molecules (Sun *et al*., 2020). The relationship between soil DOM chemodiversity and microbiome consequently plays a central role in C cycling (Li *et al*., 2021), providing a chance to uncover the molecular mechanisms underlying microbially mediated soil C processes enhanced by biochar (Ling *et al*., 2022).

We conducted a five-year field experiment in an acidic soil with a single biochar addition to overcome these potential issues and better understand the effects of biochar. The primary objective of this study was to explore how biochar amendment influences the molecular-level characteristics of soil DOM and their associations with the soil microbiome. We hypothesized that biochar-induced alterations in soil conditions, including shifts in pH and DOM components, could transform both the composition and size of the bacterial community. This transformation was also anticipated to influence the molecular structure of DOM. Specifically, i) the incorporation of SOM components from biochar application could shift soil DOM composition toward persistent molecules enriched in aromatic compounds, and ii) the characteristics of these persistent molecules would be shaped by microbes. Advanced analytical techniques such as Fourier transform ion cyclotron resonance mass spectrometry (FT-ICR MS) have unprecedented capabilities to characterize the chemodiversity of DOM (Kim *et al*., 2022). Utilizing FT-ICR MS, along with high-throughput sequencing, we investigated the molecular mechanisms underlying microbially mediated soil C processes and assessed the potential effects of biochar on soil health and C storage.

MATERIALS AND METHODS

Site description and experimental design

A field experiment was initiated in 2015 in Meihekou County in northeastern China (42.23° N, 125.46° E). According to the World Reference Base for Soil Resources (WRB), the tested soil belongs to Albic Planosol, a soil of the Albic type, which is prevalent globally and has various names in different nations (Gao, 1992). The experimental site features a temperate continental monsoon climate characterized by distinct seasons, comprising warm summers and chilly winters. The mean annual temperature is 5 °C, and the mean rainfall is approximately 700 mm, concentrated mainly from June to September.

The study had four treatments: no fertilization (NF), conventional fertilization (CF), conventional fertilization with low-rate biochar at 15 000 kg ha^{-1} (LB), and conventional fertilization with high-rate biochar at 60 000 kg ha^{-1} (HB). Conventional fertilization involved applying 90.0 kg N ha^{-1}, 70.0 kg P_2O_5 ha^{-1}, and 80.0 kg K_2O ha^{-1} during spring seeding and 90.0 kg N ha^{-1} during the jointing stage. The biochar was applied only once. The experiment followed a fully randomized block design with three replications. The plots were 30 m^2 (10 m × 3 m) and planted with maize under continuous cultivation. All plots received manual treatment. The biochar utilized in the research was generated through rice straw and husk pyrolysis at 450 °C, with a pH of 7.31, SOC content of 447.7g kg^{-1}, total N (TN) content of 15.9 g kg^{-1}, total phosphorus (P) content of 3.4 g kg^{-1}, total potassium (K) content of 31.3 g kg^{-1}, available P (AP) content of 268.0 mg kg^{-1}, and available K (AK) content of 1 800 mg kg^{-1}.

Soil sampling and chemical analyses

In July 2020, soil samples were extracted from the top 20 cm of each plot using a soil drill. Three random points per plot were sampled and composited into a single sample. Visible residues were removed prior to analysis, and the soil was sifted through a 2-mm sieve. Each composite sample was subsequently divided into three smaller subsamples. A portion of the air-dried subsample was used to determine various chemical properties, including pH, available N (AN), AP, AK, SOC, and TN. Dissolved organic C (DOC) and dissolved organic nitrogen (DON) were measured using an enviro TOC analyzer (Elementar, Hanau, Germany). Another portion of the subsample, after being passed through a 2-mm mesh, was preserved at −80 °C until DNA extraction and subsequent high-throughput sequencing analysis. The third subsample was used for the analysis of DOM.

DNA extraction, high-throughput sequencing and real-time PCR

Metagenomic DNA was extracted from 0.5 g of soil

using the FastDNA® spin kit (MP Biomedicals, Cleveland, USA) according to the manufacturer's instructions. The concentration of DNA was measured using a NanoDrop spectrophotometer (NanoDrop Technologies, Wilmington, USA). The V3–V4 region of the 16S rRNA gene was amplified *via* PCR using the universal primers 515F and 907R (Yusoff *et al*., 2013), with each primer tagged with a unique barcode for individual samples. The resulting amplicons were pooled in equal molar amounts and sequenced using an Illumina MiSeq platform (PE300) or an NovaSeq platform (PE250) (Illumina Inc., San Diego, USA) according to the standard protocols of Majorbio Bio-Pharm Technology Co., Ltd. (Shanghai, China). Initial pyrosequencing data were analyzed *via* the Quantitative Insights Into Microbial Ecology (QIIME) pipeline (version 1.9.1). Sequences were clustered into operational taxonomic units (OTUs) at a 97% similarity threshold. Taxonomic identification of bacterial and fungal OTUs was performed against the SILVA taxonomy database (Release 138). The 16S rRNA sequence data were submitted to the National Center for Biotechnology Information (NCBI) Sequence Read Archive under the accession number PRJNA1015743.

Bacterial community sizes were quantified by assessing copies of the 16S rRNA gene using the universal primer pair 515F/907R (Yusoff *et al*., 2013). Quantitative real-time PCR was performed using an ABI 7500 real-time PCR system (Applied Biosystems, Carlsbad, USA). Each reaction mixture included 16.5 μL of AceQ SYBR green qPCR master mix (2×, Thermo Fisher Scientific, Waltham, USA) and 0.8 μL of each primer (5 μmol L^{-1}, forward and reverse). Negative controls contained all the reaction components except that soil DNA was replaced with sterile water. The mean threshold cycle (Ct) from three duplicate samples was used for analysis. Copy numbers were deduced from the standard curves based on the Ct values and a regression equation.

Analysis of FT-ICR MS data

Solid-phase extraction (SPE) of DOM from soil followed the method described by Li *et al*. (2018). Initially, soil DOM was extracted using Milli-Q water in a 1:5 ratio (weight/volume) on a reciprocal shaker at 170 r min^{-1} for 8 h. After extraction, the samples were centrifuged at 2 800 × g for 10 min, and the clear supernatant was passed through a 0.45-μm mixed cellulose ester filter. Solid-phase extraction cartridges were sequentially conditioned with mass-spectrometry-grade methanol followed by 0.01 mol L^{-1} HCl (Lv *et al*., 2016). Dissolved organic matter samples were acidified to a pH of 2 and then loaded onto the prepared SPE cartridges. The DOM was thoroughly dried under a (gentle) stream of high-purity N_2 gas, eluted from the cartridges using 5 mL of methanol, and subsequently stored at −20 °C until analysis (Kellerman *et al*., 2014). The molecular composition of the SPE-DOM was examined using a 9.4 T Bruker Apex-Ultra FT-ICR MS (Bruker, Billerica, USA) equipped with an electrospray ionization (ESI) source (Bruker Apollo II) operated in negative mode (Fang *et al*., 2017). The SPE-DOM solution was prepared in methanol and delivered to the ESI source at a flow rate of 3 μL min^{-1} using a syringe pump (Wang *et al*., 2018). Mass peaks showing signal-to-noise ratios below 6 were omitted from further data analysis (Li *et al*., 2018).

Molecular intensities were normalized to the total intensities measured by FT-ICR MS, thereby yielding a relative intensity for each molecule. This normalization approach provides more detailed insights into DOM molecular composition than techniques that rely solely on the detection of molecular presence or absence (Sleighter *et al*., 2010). The H/C and O/C ratios were calculated to facilitate visual interpretation of the mass spectral data. A modified aromaticity index (AI_mod) was calculated to assess the presence of aromatic structures, whereas the double-bond equivalence (DBE) was computed to estimate the total degree of unsaturation (double bonds and rings) of each molecule formula (Li *et al*., 2018). The average molecular characteristics were estimated using magnitude-weighted C, H, O, O/C, H/C, DBE, and molecular mass (C_w, H_w, O_w, O/C_w, H/C_w, DBE_w, and MM_w, respectively). The DOM molecular-mass spectra were characterized using the absolute signal intensities of molecular formulas assigned within the mass range of 100 to 800 (Roth *et al*., 2019). Dissolved organic matter was categorized into magnitude-weighted low-molecular-mass (LMM_w, mass-to-charge ratio (m/z) 100–300), intermediate-molecular-mass (IMM_w, m/z 300–450), and high-molecular-mass fractions (HMM_w, m/z 450–800). Van Krevelen (VK) diagrams were constructed, and molecules were categorized into compound groups based on their H/C and O/C ratios derived from molecular formulas, as detailed in Table SI (see Supplementary Material for Table SI). A molecular lability boundary (MLB) was established from the FT-ICR MS molecular data, visualized using VK diagrams. This boundary separates the data into constituents that are more labile (MLB_L) and those that are less labile (D'Andrilli *et al*., 2015). Dissolved organic matter components with H/C ratios $\geqslant$ 1.5, lying above the MLB, are considered more labile, while those with H/C ratios $<$ 1.5, below the MLB, are considered less labile and more recalcitrant. The molecular stability of DOM decreases with increasing oxygenation and decreasing hydrogenation, as reflected by lower O/C and higher H/C ratios (D'Andrilli *et al*., 2015). The Gibbs free energy (ΔG°) for the carbon oxidation half-reaction in DOM molecules was computed to assess their thermodynamic characteristics (Li *et al*., 2023). A higher ΔG° for a specific organic compound signifies lower thermodynamic quality, and conversely, a lower ΔG°

suggests higher thermodynamic quality. A molecule with a high ΔG° requires more energy for oxidation, thereby indicating higher thermodynamic stability for the DOM molecule.

Network construction

Spearman's rank correlation coefficients between the relative abundances of the OTUs and DOM molecules were calculated using R (version 3.2.3). Positive ($r \geqslant 0.95$, $P \leqslant 0.05$) and negative ($r \leqslant -0.95$, $P \leqslant 0.05$) correlations were considered strong and visualized as a network using Cytoscape (version 3.7.1). In the network, OTUs and DOM molecules were designated as nodes, and significant correlations were represented as edges directed from DOM molecules (source) to OTUs (target) based on the strength of the correlation. Operational taxonomic units serving as central points in the network were defined as those connected to more than 100 molecule nodes. A network analysis was then conducted using the Network Analyzer tool in Cytoscape.

Statistical analysis

The one-way analysis of variance (ANOVA) was used to assess the impact of biochar amendment (LB and HB) on soil properties, bacterial diversity and abundance, and DOM composition. Principal coordinate analysis (PCoA) and Redundancy analysis (RDA) were performed to visualize the variations in both the bacterial community composition and DOM molecular structures among the treatments. Permutational multivariate analysis of variance (PERMANOVA) based on a Bray-Curtis matrix was employed to investigate the impact of treatments on both bacterial community composition and DOM composition. We used the glmm.hp() function from the glmm.hp package (R) for calculating the relative contributions of multiple DOM components according to hierarchical partitioning theory (Lai *et al*., 2022).

RESULTS

Soil physicochemical properties

Biochar amendment had significant main effects on soil physicochemical properties (Table SII, see Supplementary Material for Table SII). The soil properties (pH, SOC, TN, AP, AK, DOC, and DON) were significantly higher in LB and HB (biochar-amended treatments) than NF. Similarly, pH, SOC, AP, and the C to N ratio were significantly higher in HB than CF. However, AN was significantly lower in LB and HB than CF. In comparison, TN and AK did not differ significantly between CF and LB.

Soil bacterial communities and DOM

The addition of biochar had a significant impact on bacterial abundance, as assessed using gene abundance, with the highest abundance in HB (Fig. S1, see Supplementary Material for Fig. S1). Bacterial abundance was significantly higher by 58.0%, 130.9%, and 272.8% in CF, LB, and HB than NF, respectively. Bacterial diversity, evaluated using Shannon index and Chao 1, was notably lower in NF and CF (unamended treatments) than HB. Bacterial diversity and richness varied little between NF and CF. The bacterial communities were dominated by Actinobacteriota (35.3%), Proteobacteria (26.0%), Chloroflexi (13.7%), Acidobacteriota (6.4%), and Firmicutes (5.3%), in terms relative abundance (Fig. S2, see Supplementary Material for Fig. S2). Results of PCoA based on Bray-Curtis distances indicated that bacterial community composition had a significant clustering effect under biochar amendment (PERMANOVA: $R^2 = 0.392$, $P = 0.002$) based on their taxonomic characteristics (Table SIII, Fig. S3, see Supplementary Material for Table SIII and Fig. S3). Gemmatimonadota and Acidobacteriota were more abundant in LB and HB, whereas Actinobacteriota were more abundant in NF and CF ($P < 0.05$). The levels of various DOM compounds were higher, whereas the OTU richness was lower, in LB and HB than CF and NF (Fig. 1).

The DOM analysis identified 29 934 compounds, with an average of 7 484 compounds in each treatment. The Chao 1 and Shannon index of DOM molecules differed significantly in NF compared to LB and HB and were the highest in NF (Fig. S1). The β-diversity of DOM, based on Bray-Curtis distances, remained significantly different between the unamended and biochar-amended treatments (Table SIII). However, the β-diversity was notably similar between LB and HB (Fig. S3). Biochar amendment had a depleting effect on DOM composition, implied by the higher proportion of significantly depleted molecules compared with the enriched ones (1 255 *vs*. 527). The majority of the DOM compositions were lignins (59.9%), condensed aromatics (14.5%), tannins (13.0%), and protein/amino sugars (7.6%). The weighted density patterns in the van Krevelen diagrams (Fig. S4, see Supplementary Material for Fig. S4) showed notable shifts in DOM component distribution due to biochar amendment (PERMANOVA: $R^2 = 0.336$, $P = 0.004$). For example, condensed aromatics (area θ) and tannins (area μ) were more abundant in LB and HB. The percentages of MLB_L decreased from 13.57% to 7.77% with increasing biochar amendment.

Biochar amendment notably affected H_w, O_w, MM_w, H/C_w, O/C_w, DBE_w, and AI_w (Table I). Specifically, O_w, MM_w, DBE_w, and AI_w were significantly higher in LB and HB than NF and CF. Particularly noteworthy was the higher DBE_w in LB (11.13) and HB (11.23) than NF (9.68). This finding suggested a greater level of aromaticity in biochar-amended treatments, especially in HB, a trend reinforced by the lower H/C ratio (a marker of aromaticity). Conversely,

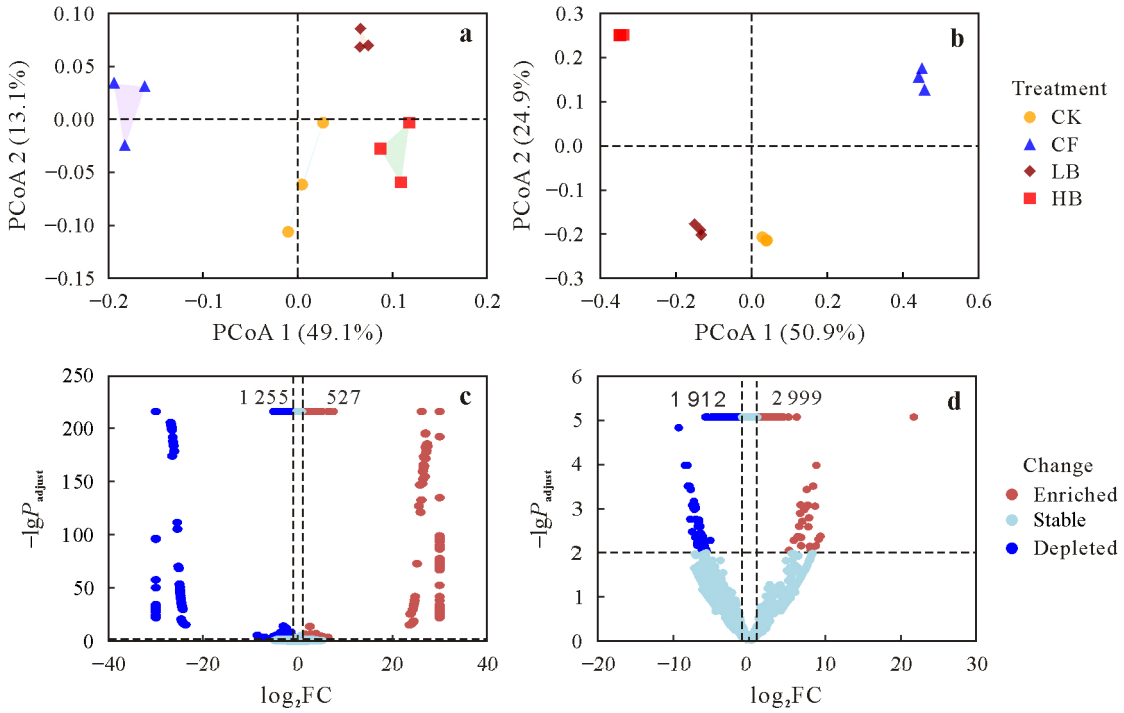

Fig. 1 Principal coordinate analysis (PCoA) of soil dissolved organic matter (DOM) molecular composition (a) and microbial community (b) based on Bray-Curtis distance in different treatments and the differential abundance analysis showing the enrichment and depletion of DOM molecules (c) and bacterial operational taxonomic units (OTUs) (d) for biochar-amended treatments compared with unamended treatments. In panels c and d, each point represents an individual molecule or OTU, the position along the x-axis represents the fold change (FC) in abundance under biochar-amended treatments compared with unamended treatments, and dashed lines indicate the significance thresholds for adjusted P value (P_{adjust}) and $\log_2$ FC. NF = no fertilization; CF = conventional fertilization; LB = conventional fertilization with low-rate biochar at 15 000 kg ha^{-1}; HB = conventional fertilization with high-rate biochar at 60 000 kg ha^{-1}.

TABLE I

Magnitude-weighted (indicated by a subscripted w) averaged characteristics[a)] of soil dissolved organic matter (DOM) in different treatments[b)]

Treatment	C_w	H_w	O_w	MM_w				H/C_w	O/C_w	DBE_w	AI_w	ΔG°
				DOM	LMM	IMM	HMM					
NF	19.01b[c)]	21.49a	8.64c	405.32c	265.49a	373.20a	521.84b	1.14a	0.477b	9.68c	0.33c	60.60a
CF	19.60a	20.45b	9.11b	415.16b	265.94a	374.63a	524.45ab	1.05b	0.484ab	10.79b	0.40b	58.02b
LB	19.51ab	19.42c	9.50a	420.86a	266.00a	375.58a	527.96a	1.00c	0.504a	11.13a	0.43a	55.63c
HB	19.48ab	19.53c	9.54a	422.28a	265.36a	375.28a	530.85a	1.01c	0.504a	11.23a	0.43a	55.48c

[a)] MM = molecular mass; DBE = double-bond equivalence; AI = aromaticity index; ΔG° = Gibbs free energy; LMM = low-molecular-mass fraction (mass-to-charge ratio (m/z) 100–300); IMM = intermediate-molecular-mass fraction (m/z 300–450); HMM = high-molecular-mass fraction (m/z 450–800).
[b)] NF = no fertilization; CF = conventional fertilization; LB = conventional fertilization with low-rate biochar at 15 000 kg ha^{-1}; HB = conventional fertilization with high-rate biochar at 60 000 kg ha^{-1}.
[c)] Averages followed by different letters within the same column are significantly different among the treatments at $P < 0.05$.

H_w and H/C_w were noticeably lower. The molecular mass was also higher in LB and HB due to the higher C_w and O_w, with an MM_w of 420.86 in LB and 422.28 in HB, compared to 405.32 in NF. The LMM_w and IMM_w were similar among the treatments, and the higher MM_w was due to the higher HMM_w, with 9.01 higher in HB compared with NF. The DOM molecules had a higher average ΔG° in NF (60.60) and CF (58.02) than in LB (55.63) and HB (55.48). The AI_w increased, but H/C_w decreased in CHO, CHON, CHOS, and CHONS compounds in LB and HB, compared to NF and CF (Table II). The MM_w of CHO, CHON, and CHOS compounds was also higher in LB and HB. The O/C_w of CHO compounds was higher in LB and HB than in NF and CF, but was similar for the other compounds. The ΔG° was lower for the CHON and CHOS compounds than for the CHO and CHONS compounds, and the ΔG° for all compounds was lower with biochar amendment.

Associations between soil bacterial species and DOM molecules

To account for the correlations between bacterial species and DOM components, a network analysis was performed to visualize the intricate associations from the taxonomic level

TABLE II

Magnitude-weighted (indicated by a subscripted w) averaged characteristics[a)] of soil dissolved organic matter (DOM) compounds in the treatments[b)]

Compound	Treatment	MM_w	H/C_w	O/C_w	DBE_w	AI_w	ΔG°
CHO	NF	411.89b[c)]	1.15a	0.447b	9.75c	0.32c	67.57a
	CF	420.96ab	1.09b	0.462b	10.47b	0.35b	65.13b
	LB	423.60ab	1.05c	0.485a	10.87a	0.38a	62.47c
	HB	425.07a	1.05c	0.486a	10.84a	0.38a	62.47c
CHON	NF	406.92b	1.06a	0.486b	10.57c	0.44c	54.13a
	CF	419.70a	0.99b	0.509a	11.40b	0.48b	51.13b
	LB	423.80a	0.95c	0.525a	11.83ab	0.51a	49.01c
	HB	427.82a	0.95c	0.513a	12.01a	0.51a	49.67bc
CHOS	NF	367.12b	1.33a	0.483a	7.51b	0.15b	50.27a
	CF	378.43ab	1.17b	0.493a	9.69a	0.24a	45.21b
	LB	386.61a	1.12b	0.492a	9.59a	0.29a	43.78b
	HB	386.52a	1.18b	0.500a	9.63a	0.26a	44.17b
CHONS	NF	398.38a	1.21a	0.586ab	7.25b	0.12c	67.10a
	CF	401.88a	0.97b	0.576b	9.58a	0.39ab	65.78a
	LB	402.43a	0.94b	0.588ab	9.63a	0.41a	63.04b
	HB	399.52a	0.95b	0.594a	9.48ab	0.41b	62.05b

[a)] MM = molecular mass; DBE = double-bond equivalence; AI = the aromaticity index; ΔG° = Gibbs free energy.
[b)] NF = no fertilization; CF = conventional fertilization; LB = conventional fertilization with low-rate biochar at 15 000 kg ha^{-1}; HB = conventional fertilization with high-rate biochar at 60 000 kg ha^{-1}.
[c)] Averages followed by different letters within the same column are significantly different among the treatments for each compound at $P < 0.05$.

of individual species to specific DOM molecules, as shown in Fig. 2. A sum of 404 OTUs and 4 309 designated DOM molecules were chosen for network analysis. Among these, 1 354 OTUs and 156 DOM molecules constituted the negative network of unamended samples, whereas 2 336 OTUs and 257 DOM molecules constituted that of biochar-amended samples. The networks were complex, comprising 3 018 and 5 029 edges, respectively, and each was divided into three subnetworks (Table SIV, see Supplementary Material for Table SIV). One particularly extensive and intricate subnetwork contained more than 500 nodes and 2 000 edges. In the unamended negative subnetworks, subnetwork a1 contained 72 OTU nodes, 787 molecule nodes, and 2 075 edges, forming three OTU centers (hubs). Subnetwork a2 contained 27 OTU nodes, 315 molecule nodes, and 660 edges, forming a network with only one large hub. Subnetwork a3 contained many single-degree OTU nodes, forming a uniformly connected complex network without a prominent hub. The OTU hubs belonged to the phyla Actinobacteriota, Bacteroidota, and Firmicutes (Table SV, see Supplementary Material for Table SV). Biochar-amended negative subnetworks had structures similar to the unamended negative subnetworks but contained more OTU hubs. For example, subnetwork b1 contained 76 OTU nodes, 1 829 molecule nodes, and 4 167 edges, forming 12 OTU hubs, which belonged to the phyla Acidobacteriota, Actinobacteriota, Bacteroidota, Chloroflexi, and Proteobacteria. In the positive networks, 1 416 OTUs and 174 DOM molecules formed the unamended networks, and 3 129 OTUs and 277 DOM molecules formed the biochar-amended networks. The selected nodes were connected by 1 590 and 3 406 edges, respectively, each of which was subdivided into three subnetworks. The unamended positive networks contained two large complex subnetworks and five OTU hubs (belonging to the phyla Actinobacteriota, Firmicutes, and Proteobacteria). Subnetwork c1 contained 75 OTU nodes, 729 molecule nodes, and 1 728 edges, and subnetwork c2 contained 66 OTU nodes, 424 molecule nodes, and 1 564 edges. The biochar-amended positive networks exhibited intricate structures, with subnetwork d1 being notably large and complex. This subnetwork comprised 165 OTU nodes, 2 730 molecule nodes, and 8 406 edges, resulting in a total of 24 OTU hubs. Most OTU hubs were mainly associated with organic components (Table SVI, see Supplementary Material for Table SVI) and belonged to the phyla Acidobacteriota, Actinobacteriota, Myxococcota, Chloroflexi, Proteobacteria, and Gemmatimonadota. The positive networks generally contained more nodes, edges, and OTU hubs than the negative networks.

The DOM molecules associated with the OTU hubs in the positive and negative subnetworks were further categorized into CHO, CHON, CHOS, and CHONS compound groups (Fig. 3). Biochar-amended subnetworks generally had higher node numbers, edge numbers, and average connectivity compared to the unamended subnetworks, indicating higher aggregation in the amended subnetworks, and the unamended subnetworks tended to be more independent (Table SVII, see Supplementary Material for Table SVII). The highest ranking OTU hubs were associated with the CHOS and CHON compounds in the unamended subnetworks and the CHO and CHON compounds in the biochar-amended subnetworks. Only the four most common OTUs from the biochar-amended and unamended subnetworks are shown in Fig. 4, whereas the others are presented in Tables SV and SVI. In the unamended subnetworks, low-molecular-

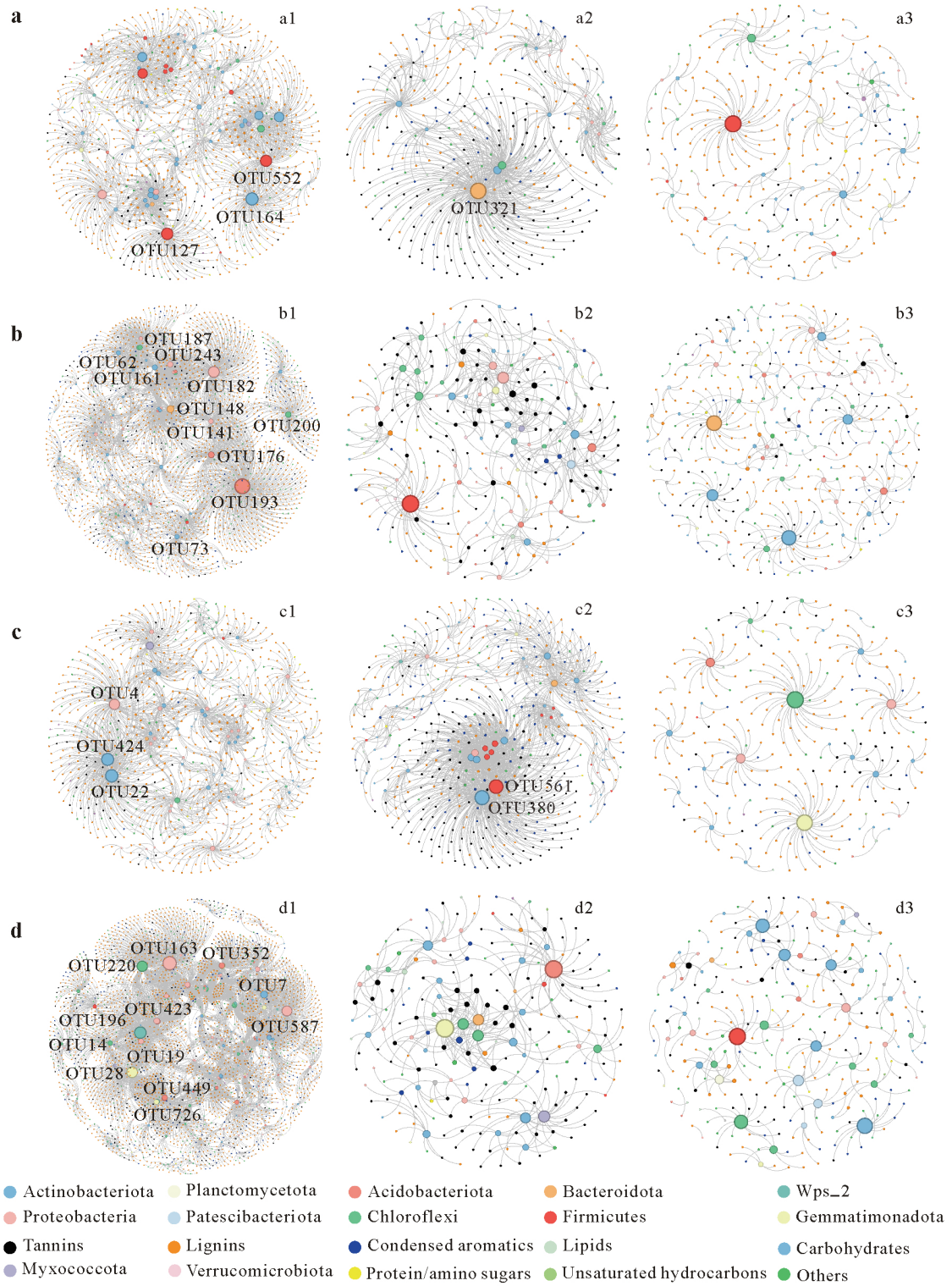

Fig. 2 Networks (divided into three subnetworks) showing the negative (a and b) and positive (c and d) associations between soil bacterial species and dissolved organic matter (DOM) molecules in unamended (a and c) and biochar-amended (b and d) treatments. Different bacterial classes and DOM components are labeled with different colors. Direct connections were established between DOM molecules and operational taxonomic units (OTUs) when the Spearman's rank correlation was strong ($|r| \geqslant 0.95$) at $P \leqslant 0.05$. Node size is proportional to the degree of connectedness. The OTU name tags are shown for nodes with more than 100 connections in the networks. Details of the network topological attributes are listed in Table SIV.

mass CHON and CHOS compounds (m/z 100–300) were considerably more abundant, whereas high-molecular-mass CHO compounds were more abundant (m/z 450–800). In the biochar-amended subnetworks, CHO and CHON compounds

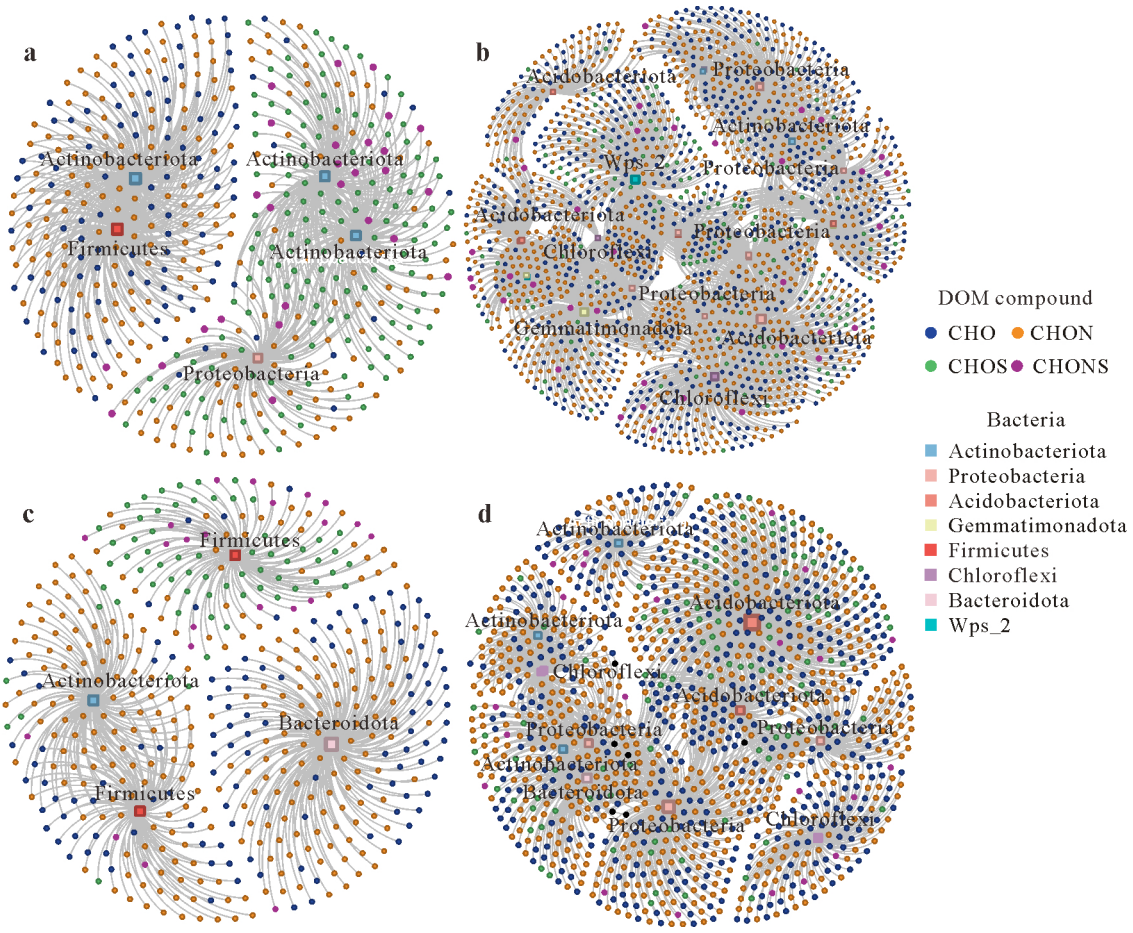

Fig. 3 Positive (a and b) and negative subnetwork layouts (c and d) showing the associations of keystone bacterial taxa and assigned dissolved organic matter (DOM) compound groups in unamended (a and c) and biochar-amended (b and d) treatments. The size of the square node is proportional to the number of connections (degree).

were more abundant and displayed similar, narrow O/C and H/C ratios within the high-molecular-mass range. The CHOS and CHONS compounds were less abundant, mainly in the intermediate-molecular-mass range (m/z 300–450).

Associations between soil bacterial community and DOM molecules

Eight magnitude-weighted parameters (C_w, H_w, O_w, MM_w, H/C_w, O/C_w, DBE_w, and AI_w) were used to obtain a more detailed characterization of the profiles of molecular chemodiversity (Fig. S5, see Supplementary Material for Fig. S5). The H_w and H/C_w were significantly negatively correlated with bacterial diversity and the soil properties, and the other magnitude-weighted parameters were significantly positively correlated with bacterial diversity and the soil properties.

The RDA was performed to estimate the contribution of DOM components to the variance in bacterial community abundance across the treatments (Fig. 5). The first two ordination axes explained 62.68% of the total variation (RDA 1 = 43.74%, RDA 2 = 18.94%). An analysis of the sample positions projected along the arrow indicated that condensed aromatics and tannins were the primary parameters affecting the bacterial communities in HB, carbohydrates and protein/amino sugars were the primary parameters in NF, and unsaturated hydrocarbons were the primary parameters in CF. Hierarchical partitioning analysis indicated that unsaturated hydrocarbons (44.54%) and condensed aromatics (16.17%) had the most significant impacts on the variation in the bacterial communities. The combination of these variables to labile DOM components explained most of the variation (40.19%), and the persistent DOM components explained 19.92% of the variation.

DISCUSSION

Biochar amendment altered soil environment, DOM structure and bacterial community

Changes in physicochemical properties and substrate utilization in the biochar-amended treatments led to compositional shifts in both soil bacterial communities and DOM molecules. The PCoA and volcano plot confirmed

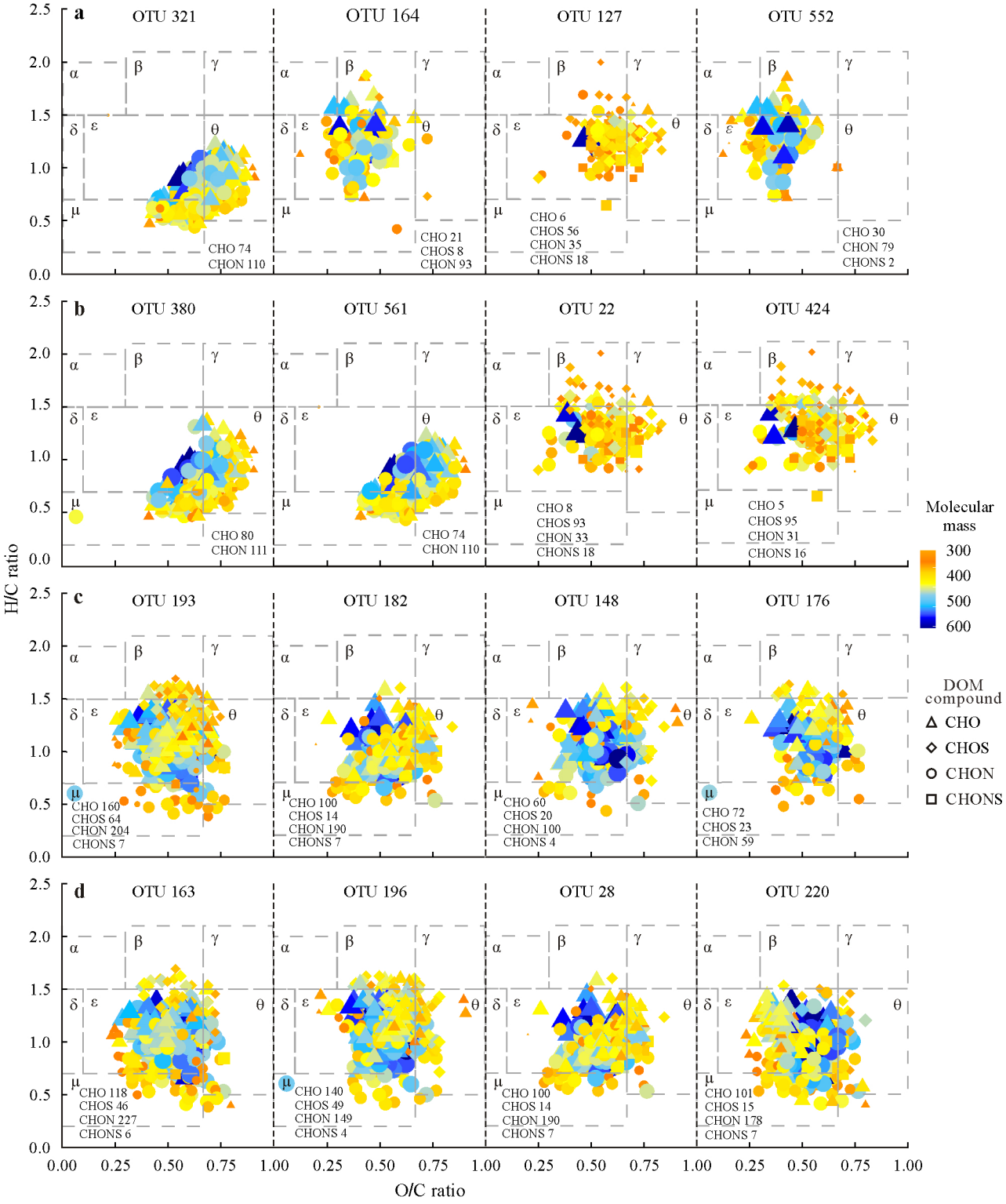

Fig. 4 Assigned soil dissolved organic matter (DOM) compound groups associated with the highest ranking operational taxonomic units (OTUs) in negative (a and c) and positive subnetworks (b and d) from unamended (a and b) and biochar-amended (c and d) treatments. The taxonomic information of the highest ranking OTUs is listed in Tables SV and SVI. The van Krevelen diagrams show the CHO, CHON, CHOS, and CHONS groups associated with each OTU. The molecular mass is also represented by the size of each point, with larger points indicating higher molecular mass. Areas α, β, γ, δ, ε, θ, and μ are clusters of lipids, protein/amino sugars, carbohydrates, unsaturated hydrocarbons, lignins, condensed aromatics, and tannins, respectively.

the significant dissimilarities between the compositions of the bacterial communities and DOM molecules in biochar-amended treatments compared with unamended treatments (Fig. 1). Specifically, biochar amendment directly shifted the

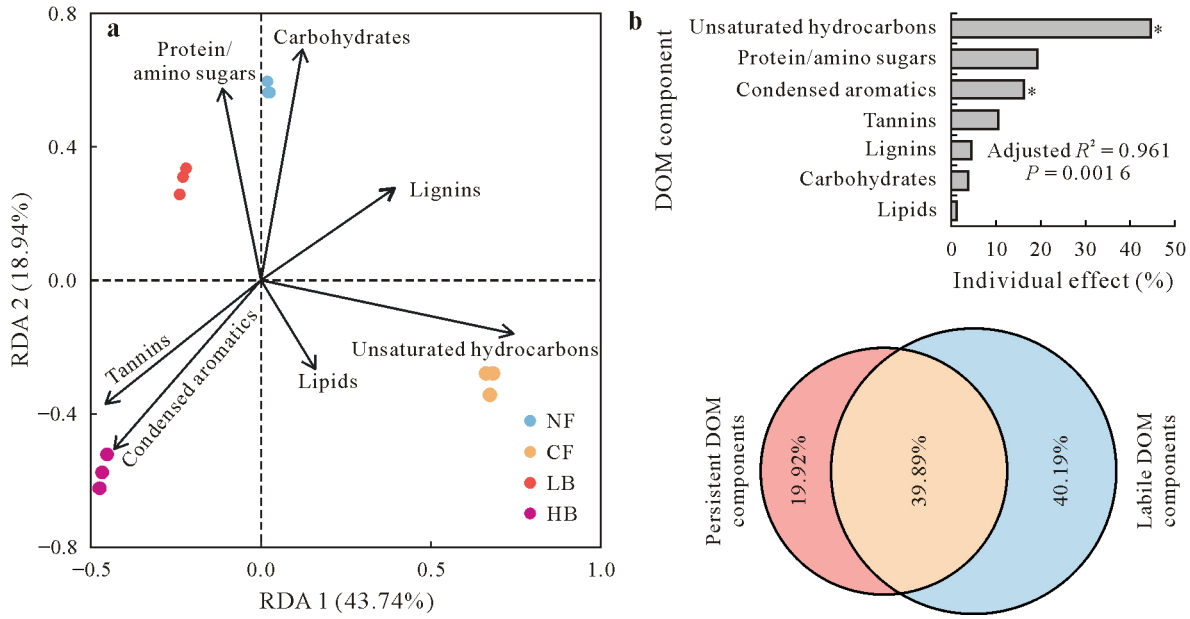

Fig. 5 Changes in dissolved organic matter (DOM) components and their impacts on bacterial communities in different treatments: redundancy analysis (RDA) showing the relationships between bacterial community structure and DOM components (a) and the hierarchical partitioning analysis showing the relative contributions of DOM components to the bacterial community (b). An asterisk * indicates significance at $P < 0.05$. NF = no fertilization; CF = conventional fertilization; LB = conventional fertilization with low-rate biochar at 15 000 kg ha^{-1}; HB = conventional fertilization with high-rate biochar at 60 000 kg ha^{-1}.

compositions of both the bacterial communities and DOM molecules, increasing the abundances of Gemmatimonadota, Actinobacteriota, and Acidobacteriota and enriching condensed aromatics and tannins. These findings suggested that variations in the responses of bacterial taxa to their preferred energy sources for metabolic requirements led to the competitive dominance of specific microbial groups (Chen *et al*., 2021), further influencing the overall microbial community structure (Zhao *et al*., 2019).

In the biochar-amended treatments, C_w, DBE_w, and AI_w notably increased, but H/C_w decreased (a marker of aromaticity), especially in HB, compared with unamended treatments (Table I). The positive correlation between pH and DBE_w suggested an elevated presence of C=C unsaturation as pH increased. Soil pH was significantly correlated positively with O_w, O/C_w, MM_w, and AI_w but negatively with H_w and H/C_w. Increased pH was associated with the higher aromatic nature of the DOM molecules in the biochar-amended soil (D'Andrilli *et al*., 2015), and DOM in soil conditions characterized by higher acidity contained more C-saturated compounds (such as carbohydrates and proteins), rendering them more prone to inherent degradability. In contrast, the increase in aromaticity could be attributed to the presence of recalcitrant C compounds in the biochar, which resist decomposition and contribute to the stability of SOM (Ling *et al*., 2022). For example, the enrichment of condensed aromatics and tannins in this study suggests that biochar amendment promotes their accumulation in the SOM pool. These results indicated that biochar addition transformed the composition of soil DOM, favoring molecules with more C, higher molecular mass and stability, and higher aromaticity, but reducing the percentage of MLB_L (Fig. S4). This stabilizing effect can lead to soil C accumulation over time, thereby contributing to C sequestration and the long-term improvement of soil fertility.

Biochar amendment resulted in a notable increase in MM_w, indicating a shift from low- and medium-molecular-mass compounds to more significant high-molecular-mass ones. The MM_w of CHONS compounds and the saturation of CHOS and CHONS compounds remained largely unchanged following the addition of biochar, implying that the overall increase in MM_w was primarily due to an increase in the abundance of the high-molecular-mass CHO and CHON compounds, specifically those not containing sulfur atoms. The chemical characteristics of DOM were also similar in LB and HB. Biochar amendment may have led to the homogenization of community similarity. Dissolved organic matter molecules are consistently transformed into refractory compounds (Li *et al*., 2019). Even after five years of biochar amendment, the DOM molecules in LB and HB remain less thermodynamically stable (*i.e*., $\Delta G°$) than those in NF and CF, making them more readily accessible to microbes (Zhang *et al*., 2021). The emerging high-molecular-mass compounds in biochar-amended treatments may signify the generation of new molecules by the decomposer community, such as microbial products, rather than the products of random polymerization, thereby contributing to the persistence of DOM

through its continuous decomposition, recycling, and renewal (Roth *et al*., 2019). The CHON and CHOS compounds also had lower thermodynamic stabilities in the subnetwork groups. Consequently, the higher transformation potential of DOM in the biochar-amended treatments likely promoted the homogenization of DOM composition, primarily through the transformation of CHON and CHOS compounds and the formation of high-molecular-mass CHO and CHON compounds.

The modifications to SOM structure were not only caused by the physical mixture of an amendment with the soil, but also influenced by other factors, such as microbial decomposition and transformation (Zheng *et al*., 2021). The DOM in LB and HB had similar chemical characteristics, indicating that microbes can use and convert biochar into DOM products, which are consistently retained in the soil. Do these findings suggest that most of the DOM in soil amended with biochar is characterized by its relative stability and the presence of comparable DOM constituents that are not readily accessible to microorganisms? Although data on alterations in microbial communities and DOM composition are available, they do not fully account for the decomposition and transformation of biochar. This is because its decomposition is not influenced by one microbial species but by the collaborative efforts of many species. Further analyses are required to identify intricate associations and patterns of microbial species and DOM molecules and to understand how these associations respond to biochar addition.

Soil bacterial groups that were associated with DOM components

The consumption and accumulation of DOM are due to the interaction between a heterogeneous bacterial community and DOM molecules. An intriguing question in microbial ecology involves the potential existence of a connection between bacterial populations and chemical compounds. Network analyses visually represent the intricate associations among numerous bacterial species and DOM molecules, aiding us in identifying pivotal microbial species or in discerning patterns of interaction (Zhao *et al*., 2019). A negative correlation in a co-occurrence network indicates the affinity of microbes for specific compounds, indicating their use of the compounds, but a positive correlation suggests an environmental niche that has favored the assemblage of a particular soil microbiome, leading to the accumulation of specific chemical compounds by microbes (Ling *et al*., 2022). The fundamental shifts in the structural characteristics of co-occurrence networks in our study paralleled the changes in both the bacterial communities and DOM compositions. The networks formed by biochar amendment, characterized by higher average connectivity, exhibited a higher level of intricate interconnections among the microbes (Fig. 2). The positive correlations between the bacterial and DOM species were approximately twice as strong as the negative correlations. These findings suggest that the DOM in the biochar-amended treatments contributed more to the bacteria than to their consumption of DOM. Conversely, DOM remained in equilibrium in the unamended treatments; the strengths of the positive and negative correlations were nearly equal.

The networks in this study were classified into three main groups based on their complexity, each of which contained many OTU-central nodes (a single OTU node connected to multiple DOM nodes), and nodes with more than 100 connections were defined as keystone taxa in the networks. The keystone taxa, with their broader and multiple connections to compounds in the networks (Chen *et al*., 2019), could serve as valuable targets for further functional studies on bacteria involved in DOM decomposition, because they can generate and/or utilize various DOM molecules in both positive and negative networks. Biochar amendment shifted the bacterial community composition, with the classes Acidobacteriae, Alphaproteobacteria, Gemmatimonadetes, and Actinobacteria emerging as keystone taxa. Labile components showed a strong and negative correlation with the classes Alphaproteobacteria, Acidobacteriae, and Gemmatimonadetes, indicating their ability to utilize these readily degradable molecules. Alphaproteobacteria, one of the most abundant classes across all samples, may have been favoured in biochar-amended soils due to their preference for higher C and nutrient availability (Koyama *et al*., 2014). Gemmatimonadetes may be able to adapt and survive in acidic conditions, and the growth of the isolated strain *Gemmatimonas aurantiaca* T-27 has been reported to improve within the pH range of 6.5–9.0 (Luo *et al*., 2013).

The rise in soil pH induced by biochar addition promoted the growth and an eightfold surge in the prevalence of the class Gemmatimonadetes (Fig. S2), leading to the breakdown of DOM. Nevertheless, our findings for Alphaproteobacteria and Gemmatimonadetes differed from those of previous research. Earlier studies had primarily indicated that these two bacterial groups were better suited for decomposing refractory organic matter (Whitman *et al*., 2019), such as polyaromatic components in soils, but we found a significant negative correlation between the abundances of Alphaproteobacteria and Gemmatimonadetes and labile DOM components. These microbes may utilize both labile and recalcitrant DOM compounds under different environmental conditions, reflecting their metabolic flexibility and ability to exploit various C sources. For example, several members of Alphaproteobacteria, such as the genus *Microvirga*, as well as functional groups like methanotrophs and methylotrophs, occupy diverse habitats and display broad substrate utilization capabilities (Zhao *et al*., 2019). Additionally, despite the

high biochar amendment that increased soil pH, the overall environment remained acidic. This persistent acidity is one reason why the class Acidobacteriae became a keystone taxon, as it can alter the structure and composition of cellular membranes to maintain integrity under acidic conditions (Baker *et al*., 2024). Acidobacteria are typically associated with an ecological K-strategy; however, they can efficiently utilize unstable substances in acidic environments where many other bacteria are dormant (Hou *et al*., 2024). The class Actinobacteria was more prevalent in biochar-amended treatments, and its abundance showed a negative association with the occurrence of recalcitrant DOM components such as tannins and condensed aromatics. The ability of Actinobacteria to break down persistent polycyclic aromatic hydrocarbons is well documented (Zhu *et al*., 2019). These hydrocarbons play a pivotal role in shaping microbial response to biochar amendment. The presence of Actinomycetes in the biochar decomposition can be attributed to their mycelium-like morphology, which enhances contact with organic C and thus facilitates its decomposition (Jeewani *et al*., 2020).

The keystone bacterial taxa in the biochar-amended subnetworks were mostly associated with the CHO and CHON groups, characterized by similar, narrow O/C and H/C ratios within the high-molecular-mass range (Figs. 3 and 4). This finding also reconfirms, from a microbiological perspective, that high-molecular-mass CHO and CHON compounds were the main components of the DOM molecules in biochar-amended treatments. External bacterial membranes contain transport channels, often known as porins, which allow molecules smaller than 600 Da to diffuse through, facilitating the uptake of smaller molecules (Vergalli *et al*., 2020). The preferential elimination of small DOM molecules could consequently be associated with the microbial uptake through these channels (Wagner *et al*., 2020). Microbial uptake plays a crucial role in influencing the variations in molecular mass in DOM, due to the increase in microbial abundance with biochar amendment. The increases in DOC and DON contents following biochar addition could also result from microbial processing of DOM, which involves either the microbial recycling of C and N or the preservation of molecular structures containing these elements. The increase in high-molecular-mass substances in biochar-amended soils indicates the formation of new microbial DOM products with higher average molecular mass. Interestingly, a recent study has reported that freshly produced DOM from primary producers is usually dominated by low-molecular-mass compounds (de Melo *et al*., 2020). In contrast, refractory DOM exhibits a pronounced shift toward higher molecular masses. This shift suggests that the decrease in small-molecule abundance is attributed to both the ongoing breakdown of partially biochar-sourced DOM and the microbial reconstruction of new DOM molecules, potentially rich in tannins, which may account for the increase in DOC content. The increase in DON content was also likely more attributable to condensed aromatics, particularly those rich in nitrogenous molecular structures.

Associations of soil DOM components with bacterial community

The association between bacterial groups and DOM components in biochar-amended treatments provides valuable insights into the mechanisms underlying the dynamics of soil microbial communities and nutrient cycling. We used an RDA to further assess the contribution of DOM components to the variation in bacterial community composition across the treatments (Fig. 5). Results from the RDA and hierarchical partitioning analyses indicated that specific DOM components, including condensed aromatics and unsaturated hydrocarbons, significantly influenced the bacterial communities. Condensed aromatics, which primarily affect bacterial community compositions in soils with high amounts of biochar amendment, and unsaturated hydrocarbons, which mainly affect bacterial community compositions in soils treated solely with chemical fertilizer, are persistent and labile components of DOM. Soil microbes initially consume labile DOM components, and persistent components are used only after the labile components are almost depleted (Yuan *et al*., 2017). This microbial preference for novelty slows the overall turnover of SOM, leading to the persistence of aged C in the soil. The majority of the molecules that increased in abundance in soils treated with biochar (compared to NF and CF) were recalcitrant components, with a minor decrease in labile components following five years of biochar amendment. Indeed, this mechanism was also one of the mechanisms by which biochar contributes to the C sequestration (Sun *et al*., 2020). The significant contribution of condensed aromatics to the bacterial community, however, also indirectly suggested that microbes would continue to use recalcitrant DOM. The extended retention (slower turnover rate) of recalcitrant SOM has been attributed to oligotrophic microenvironments (Ling *et al*., 2022), independent of the potential mineralization of substrates. This phenomenon was part of a persistence mechanism rather than a mechanism of chemical fixation, suggesting that soil C sequestration was primarily driven by biophysical processes instead of chemical transformations. These findings provide substantial support to the notion that the extended aging of biochar in a field setting could lead to a higher retention of aromatic and condensed aromatic compounds in the soil, consequently inducing a more pronounced alteration in the composition of soil-derived DOM (Cai *et al*., 2020). Lignins also constituted the largest proportion of DOM, which is traditionally considered complex and recalcitrant, posing challenges for microbes to use (Zhang *et al*., 2022). Our study focused only

on bacteria, so the limited production of lignin-degrading enzymes by only a few fungal types (Tuomela *et al*., 2000) resulted in insignificant findings regarding lignins. Molecular identification, with a particular emphasis on analyzing the molecular compositions and their distinctive characteristics, is thus crucial for gaining a deeper understanding of SOM.

Our findings offer crucial insights into the interaction between biochar amendment, soil health, and ecosystem functionality. The observed shifts in soil microbial communities and the enhanced stability of DOM underscore the importance of biochar in promoting resilient soil ecosystems. By fostering the growth of beneficial microbial taxa and increasing the abundance of stable organic compounds, biochar can significantly enhance SOC storage and improve SOM structure. The integration of biochar into land management practices can optimize C sequestration through the promotion of diverse microbial interactions and the stabilization of organic matter. Strategies that focus on enhancing microbial diversity and increasing organic inputs will likely synergistically improve SOC dynamics and overall soil health. Furthermore, the distinct roles of high-molecular-mass DOM in supporting microbial activity suggest that targeted approaches could enhance the retention of SOC, thereby maximizing its storage potential. Future research should aim to explore the intricate relationships among biochar, microbial communities, and SOC dynamics to identify potential synergies and trade-offs with other ecosystem services. This study provides a foundational understanding of how biochar influences soil health, C storage, and microbial interactions, guiding the development of science-based land management strategies that enhance sustainable ecosystem resilience and effectively mitigate climate change.

CONCLUSIONS

Our study provides novel insights into the impact of biochar amendment on soil DOM structure and its interaction with the bacterial community. Biochar amendment not only increased soil C content and pH but also enhanced the recalcitrant DOM, ultimately increasing the retention of DOM. These effects were primarily achieved by augmenting the aromaticity and molecular mass of DOM molecules while reducing their C saturation, leading to the prevalence of condensed aromatics and tannins in the DOM components. More importantly, biochar amendment noticeably lowered the thermodynamic stability of DOM, leading to a more homogeneous composition primarily promoting the formation of high-molecular-mass CHO and CHON compounds. From a microbiological perspective, this study further substantiated that high-molecular-mass CHO and CHON compounds in the biochar-amended co-occurrence networks were closely associated with the bacterial keystone taxa and represent the principal components of DOM molecules. While these findings are fundamental, the consequences of the complex interactions between the associated bacteria and DOM, spanning from the species level to the molecular level, will be important for effective environmental and agricultural management.

DECLARATION OF COMPETING INTEREST

The authors declare that they have no known competing financial interests or personal relationships that could have appeared to influence the work reported in this paper.

ACKNOWLEDGEMENTS

This research is supported by the National Key Research and Development Program of China (No. 2022YFD 1500100), the Strategic Priority Research Program of Chinese Academy of Sciences (No. XDA28070100), and the Earmarked Fund for China Agriculture Research System (No. CARS-04).

SUPPLEMENTARY MATERIAL

Supplementary material for this article can be found in the online version.

REFERENCES

Baker N R, Zhalnina K, Yuan M T, Herman D, Ceja-Navarro J A, Sasse J, Jordan J S, Bowen B P, Wu L Y, Fossum C, Chew A, Fu Y, Saha M, Zhou J Z, Pett-Ridge J, Northen T R, Firestone M K. 2024. Nutrient and moisture limitations reveal keystone metabolites linking rhizosphere metabolomes and microbiomes. *Proc Natl Acad Sci USA*. **121**: e2303439121.

Cai W, Du Z L, Zhang A P, He C, Shi Q, Tian L Q, Zhang P, Li L P, Wang J J. 2020. Long-term biochar addition alters the characteristics but not the chlorine reactivity of soil-derived dissolved organic matter. *Water Res*. **185**: 116260.

Chen L J, Jiang Y J, Liang C, Luo Y, Xu Q S, Han C, Zhao Q G, Sun B. 2019. Competitive interaction with keystone taxa induced negative priming under biochar amendments. *Microbiome*. **7**: 77.

Chen Z Y, Kumar A, Fu Y Y, Singh B P, Ge T D, Tu H, Luo Y, Xu J M. 2021. Biochar decreased rhizodeposits stabilization via opposite effects on bacteria and fungi: Diminished fungi-promoted aggregation and enhanced bacterial mineralization. *Biol Fertil Soils*. **57**: 533–546.

D'Andrilli J, Cooper W T, Foreman C M, Marshall A G. 2015. An ultrahigh-resolution mass spectrometry index to estimate natural organic matter lability. *Rapid Commun Mass Spectrom*. **29**: 2385–2401.

de Melo M L, Kothawala D N, Bertilsson S, Amaral J H, Forsberg B, Sarmento H. 2020. Linking dissolved organic matter composition and bacterioplankton communities in an Amazon floodplain system. *Limnol Oceanogr*. **65**: 63–76.

Ding Y, Shi Z Q, Ye Q T, Liang Y Z, Liu M Q, Dang Z, Wang Y J, Liu C X. 2020. Chemodiversity of soil dissolved organic matter. *Environ Sci Technol*. **54**: 6174–6184.

Fang Z, He C, Li Y Y, Chung K H, Xu C M, Shi Q. 2017. Fractionation and characterization of dissolved organic matter (DOM) in refinery wastewater by revised phase retention and ion-exchange adsorption solid phase extraction followed by ESI FT-ICR MS. *Talanta*. **162**: 466–473.

Feng Z J, Fan Z L, Song H P, Li K L, Lu H N, Liu Y, Cheng F Q. 2021. Biochar induced changes of soil dissolved organic matter: The release

and adsorption of dissolved organic matter by biochar and soil. *Sci Total Environ*. **783**: 147091.

Fu Y Y, Luo Y, Auwal M, Singh B P, Van Zwieten L, Xu J M. 2022. Biochar accelerates soil organic carbon mineralization *via* rhizodeposit-activated Actinobacteria. *Biol Fertil Soils*. **58**: 565–577.

Gao Z Q. 1992. Comprehensive Management of Agriculture, Forestry and Animal Husbandry for Albic Soils in Sanjiang (Heilong, Songhua and Wusuli Rivers) Plain (in Chinese). China Forestry Publishing House, Beijing.

Han L F, Liu B B, Luo Y, Chen L Y, Ma C X, Xu C, Sun K, Xing B S. 2024. Quantifying the negative effects of dissolved organic carbon of maize straw-derived biochar on its carbon sequestration potential in a paddy soil. *Soil Biol Biochem*. **196**: 109500.

Hou X Y, Qiao W T, Gu J D, Liu C Y, Hussain M M, Du D L, Zhou Y, Wang Y F, Li Q. 2024. Reforestation of *Cunninghamia lanceolata* changes the relative abundances of important prokaryotic families in soil. *Front Microbiol*. **15**: 1312286.

Jeewani P H, Gunina A, Tao L, Zhu Z K, Kuzyakov Y, Van Zwieten L, Guggenberger G, Shen C C, Yu G H, Singh B P, Pan S T, Luo Y, Xu J M. 2020. Rusty sink of rhizodeposits and associated keystone microbiomes. *Soil Biol Biochem*. **147**: 107840.

Kellerman A M, Dittmar T, Kothawala D N, Tranvik L J. 2014. Chemodiversity of dissolved organic matter in lakes driven by climate and hydrology. *Nat Commun*. **5**: 3804.

Kim S, Kim D, Jung M J, Kim S. 2022. Analysis of environmental organic matters by ultrahigh-resolution mass spectrometry—A review on the development of analytical methods. *Mass Spectrom Rev*. **41**: 352–369.

Koyama A, Wallenstein M D, Simpson R T, Moore J C. 2014. Soil bacterial community composition altered by increased nutrient availability in Arctic tundra soils. *Front Microbiol*. **5**: 516.

Lai J S, Zou Y, Zhang S, Zhang X G, Mao L F. 2022. glmm.hp: An R package for computing individual effect of predictors in generalized linear mixed models. *J Plant Ecol*. **15**: 1302–1307.

Li T, Li P F, Qin W, Wu M, Saleem M, Kuang L, Zhao S, Tian C Y, Li Z P, Jiang J D, Chen K, Wang B Z. 2023. Fertilization weakens the ecological succession of dissolved organic matter in paddy rice rhizosphere soil at the molecular level. *Environ Sci Technol*. **57**: 19782–19792.

Li X M, Sun G X, Chen S C, Fang Z, Yuan H Y, Shi Q, Zhu Y G. 2018. Molecular chemodiversity of dissolved organic matter in paddy soils. *Environ Sci Technol*. **52**: 963–971.

Li X M, Chen Q L, He C, Shi Q, Chen S C, Reid B J, Zhu Y G, Sun G X. 2019. Organic carbon amendments affect the chemodiversity of soil dissolved organic matter and its associations with soil microbial communities. *Environ Sci Technol*. **53**: 50–59.

Li Y, Heal K, Wang S Z, Cao S, Zhou C F. 2021. Chemodiversity of soil dissolved organic matter and its association with soil microbial communities along a chronosequence of Chinese fir monoculture plantations. *Front Microbiol*. **12**: 729344.

Ling L, Luo Y, Jiang B, Lv J T, Meng C M, Liao Y H, Reid B J, Ding F, Lu Z J, Kuzyakov Y, Xu J M. 2022. Biochar induces mineralization of soil recalcitrant components by activation of biochar responsive bacteria groups. *Soil Biol Biochem*. **172**: 108778.

Luo Y, Durenkamp M, De Nobili M, Lin Q, Devonshire B J, Brookes P C. 2013. Microbial biomass growth, following incorporation of biochars produced at 350 °C or 700 °C, in a silty-clay loam soil of high and low pH. *Soil Biol Biochem*. **57**: 513–523.

Lv J T, Zhang S Z, Wang S S, Luo L, Cao D, Christie P. 2016. Molecular-scale investigation with ESI-FT-ICR-MS on fractionation of dissolved organic matter induced by adsorption on iron oxyhydroxides. *Environ Sci Technol*. **50**: 2328–2336.

Roth V N, Lange M, Simon C, Hertkorn N, Bucher S, Goodall T, Griffiths R I, Mellado-Vázquez P G, Mommer L, Oram N J, Weigelt A, Dittmar T, Gleixner G. 2019. Persistence of dissolved organic matter explained by molecular changes during its passage through soil. *Nat Geosci*. **12**: 755–761.

Sleighter R L, Liu Z F, Xue J H, Hatcher P G. 2010. Multivariate statistical approaches for the characterization of dissolved organic matter analyzed by ultrahigh resolution mass spectrometry. *Environ Sci Technol*. **44**: 7576–7582.

Sun K, Han L F, Yang Y, Xia X H, Yang Z F, Wu F C, Li F B, Feng Y F, Xing B S. 2020. Application of hydrochar altered soil microbial community composition and the molecular structure of native soil organic carbon in a paddy soil. *Environ Sci Technol*. **54**: 2715–2725.

Tuomela M, Vikman M, Hatakka A, Itävaara M. 2000. Biodegradation of lignin in a compost environment: A review. *Bioresour Technol*. **72**: 169–183.

Underwood G J C, Michel C, Meisterhans G, Niemi A, Belzile C, Witt M, Dumbrell A J, Koch B P. 2019. Organic matter from Arctic sea-ice loss alters bacterial community structure and function. *Nat Climate Change*. **9**: 170–176.

Vergalli J, Bodrenko I V, Masi M, Moynié L, Acosta-Gutiérrez S, Naismith J H, Davin-Regli A, Ceccarelli M, van den Berg B, Winterhalter M, Pagès J M. 2020. Porins and small-molecule translocation across the outer membrane of Gram-negative bacteria. *Nat Rev Microbiol*. **18**: 164–176.

Wagner S, Schubotz F, Kaiser K, Hallmann C, Waska H, Rossel P E, Hansman R, Elvert M, Middelburg J J, Engel A, Blattmann T M, Catalá T S, Lennartz S T, Gomez-Saez G V, Pantoja-Gutiérrez S, Bao R, Galy V. 2020. Soothsaying DOM: A current perspective on the future of oceanic dissolved organic carbon. *Front Mar Sci*. **7**: 341.

Wang L, Chen D J, Zhu L Z. 2023. Biochar carbon sequestration potential rectification in soils: Synthesis effects of biochar on soil CO_2, CH_4 and N_2O emissions. *Sci Total Environ*. **904**: 167047.

Wang X, Wang J, Li K X, Zhang H F, Yang M. 2018. Molecular characterization of effluent organic matter in secondary effluent and reclaimed water: Comparison to natural organic matter in source water. *J Environ Sci*. **63**: 140–146.

Weng Z, Van Zwieten L, Singh B P, Tavakkoli E, Joseph S, Macdonald L M, Rose T J, Rose M T, Kimber S W L, Morris S, Cozzolino D, Araujo J R, Archanjo B S, Cowie A. 2017. Biochar built soil carbon over a decade by stabilizing rhizodeposits. *Nat Climate Change*. **7**: 371–376.

Whitman T, Whitman E, Woolet J, Flannigan M D, Thompson D K, Parisien M A. 2019. Soil bacterial and fungal response to wildfires in the Canadian boreal forest across a burn severity gradient. *Soil Biol Biochem*. **138**: 107571.

Yuan Z W, He C, Shi Q, Xu C M, Li Z S, Wang C Z, Zhao H Z, Ni J R. 2017. Molecular insights into the transformation of dissolved organic matter in landfill leachate concentrate during biodegradation and coagulation processes using ESI FT-ICR MS. *Environ Sci Technol*. **51**: 8110–8118.

Yusoff M Z M, Hu A Y, Feng C J, Maeda T, Shirai Y, Hassan M A, Yu C P. 2013. Influence of pretreated activated sludge for electricity generation in microbial fuel cell application. *Bioresour Technol*. **145**: 90–96.

Zhang J W, Feng Y Z, Wu M, Chen R R, Li Z P, Lin X G, Zhu Y G, Delgado-Baquerizo M. 2021. Evaluation of microbe-driven soil organic matter quantity and quality by thermodynamic theory. *mBio*. **12**: e03252-20.

Zhang L, Sun Q X, Dou Q H, Lan S, Peng Y Z, Yang J C. 2022. The molecular characteristics of dissolved organic matter in urbanized river sediments and their environmental impact under the action of microorganisms. *Sci Total Environ*. **827**: 154289.

Zhao Z, Gonsior M, Schmitt-Kopplin P, Zhan Y C, Zhang R, Jiao N Z, Chen F. 2019. Microbial transformation of virus-induced dissolved organic matter from picocyanobacteria: Coupling of bacterial diversity and DOM chemodiversity. *ISME J*. **13**: 2551–2565.

Zheng X B, Dong J X, Zhang W H, Xiang J, Yin X S, Han L F. 2021. Biogas residue biochar shifted bacterial community, mineralization, and molecular structure of organic carbon in a sandy loam Alfisol. *GCB Bioenergy*. **13**: 838–848.

Zhu X M, Mao L J, Chen B L. 2019. Driving forces linking microbial community structure and functions to enhanced carbon stability in biochar-amended soil. *Environ Int*. **133**: 105211.